Fragility Estimates for RC and PT Flat Slab-Column Connections Subjected to Lateral Drifts

A.R. Vijaya Narayanan
Indian Institute of Technology Madras, India

D. C. Rai
Indian Institute of Technology Kanpur, India

SUMMARY:
Fragility curves are developed using experimental data available in literature for, RC slab-column connections without shear reinforcement, with shear reinforcement other than shear-studs, with shear-studs as shear reinforcement, and PT slab-column connections without shear reinforcement. Fragility curves are developed for three defined limit states, corresponding to yield, peak and post peak states. Fragility curves developed without considering the specimen-to-specimen variability results in a poor estimation of vulnerability. Effects of specimen-to-specimen variability and epistemic errors are included in the development of fragility curves. Specimen-to-specimen variability is included by incorporating the gravity shear ratio. The seismic performance of PT slab-column connection is better only marginally than that of its RC counterpart. Use of shear reinforcement significantly reduces the vulnerability of connections. The use of shear stud for shear reinforcement is observed to be more effective than stirrups.

Keywords: Flat Plate, Drift Limit, Vulnerability Assessment, Fragility curve, Damage

1. INTRODUCTION

Flat-slab systems are increasingly becoming popular due to factors such as, simple formwork, reduced construction cost, increased open office space and, shorter story height as a result of shallow profile have propelled the usage flat-slab system. In addition, with the use of Post Tensioned (PT) system, it has been observed that increased clear span can be achieved at significantly reduced depth of slab. The reduction in slab depth at each floor level leads to reduced base shear and overturning moment. However, past failures and inherent deficiencies, such as reduced lateral stiffness coupled with the likelihood of punching shear failure has raised concerns over the use of flat-slab systems in high seismic regions.

Often flat slab systems are supplemented with lateral resisting systems to enhance the lateral stiffness and strength. Consequently, slab-column connections are not designed to be a part of lateral load resisting system in moderate and high seismic regions. Instead, they are required to resist the imposed lateral drift, arising from the deformation of the lateral resisting system when subjected to seismic action. In practice, depending upon functional requirement and building configuration, several types of slab-column connections are in use, namely (a) reinforced concrete slab-column connection, (b) post tensioned slab-column connection, (c) reinforced concrete slab-column connection with shear reinforcement, and (d) post tensioned slab-column connection with shear reinforcement. Over the last three decades, numerous experiments have been carried out to evaluate force-deformation characteristics of each of the slab-column connection, mentioned above. Based on experimental investigations, it is evident that all types of slab-column connections are highly susceptible to brittle punching shear failure when subjected to lateral drift. Further, it is observed that the force-deformation characteristics significantly vary depending on the type of slab-column connection [Megally *et al.*, 1994, Kang *et al.*, 2007].

The objective of the current study is to compare different types of slab-column connections based on its seismic vulnerability and to systematically evaluate the possible damage that could be induced to them when subjected to lateral drifts. One of the most simple and elegant methodology to evaluate vulnerability analysis of the slab-column connection is through the generation of fragility curves. Through the developed fragility curves, the probability of damage to the connection, or the probability of the connection reaching a specified damage state, could be evaluated. For evaluation of seismic vulnerability, the slab-column connections are classified into five different categories, namely:

TYPE- A: RC slab-column connections without shear reinforcement,
TYPE- B: RC slab-column connection with shear reinforcement other than shear-studs,
TYPE- C: RC slab-column connection with shear-studs (SSR) as shear reinforcement,
TYPE- D: PT slab-column connections without shear reinforcement, and
TYPE- E: PT slab-column connection with shear reinforcement.

Throughout this study, the terminology ductile and non-ductile connection refers to connections with and without any shear reinforcement, respectively. Various methods available for the development of fragility curve are from (a) damage observed during past earthquakes, (b) experimental data, and (c) engineering analysis. In this study, the fragility curves for various systems have been developed based on experimental data compiled from the literature. The three basic steps involved in developing fragility curve are:
(1) Defining the damage state as a function of drift capacity,
(2) Compiling the drift capacity based on the damage state delineated from various experimental results, and
(3) Developing the fragility curve based on the data set compiled.

2. DAMAGE STATE AND EXPERIMENTAL RESULTS

For the current study, damage states for all slab-column connection were developed as a function of drift. In total three damage states are outlined. Fig. 2.1 represents the drift associated with each damage state.

The first damage state, *DS 2*, corresponds to the drift where the first yielding of reinforcement occurs within the connection. This damage state also indicates the drift at which the slab-column connection would have undergone permanent residual plastic displacement resulting in extensive cracking and which would require some level of retrofitting. The definition adopted by Pan and Mohele [1989] was utilized, to set down the drift associated with *DS 2*.

The second damage state, *DS 3*, corresponds to the drift at which the slab-column connection attains it peak lateral load carrying capacity. As most of the slab-column connections fail due to shear, this damage state 3, corresponds to the drift where punching shear failure occurs. When the slab-column connection fails through shear, the failure would be characterized through the formation of tangential cracking around the slab-column critical perimeter resulting in considerable spalling of concrete would be evident.

The third damage state, *DS 4*, corresponds to the drift, where the lateral load carrying capacity reduces to 80% of its peak capacity. This state indicates the residual capacity of the slab-column connection after its peak load carrying capacity is reached. Failure of slab-column connection under punching shear mode is generally sudden, and as a result the drift associated with damage state DS3 could be numerically equal to the drift observed at *DS 4*. On the other hand, when the slab-column connection fails through the flexural-punching mode, the drift limit associated with *DS 4* state would be significantly higher than the drift limit corresponding to *DS 3* states.
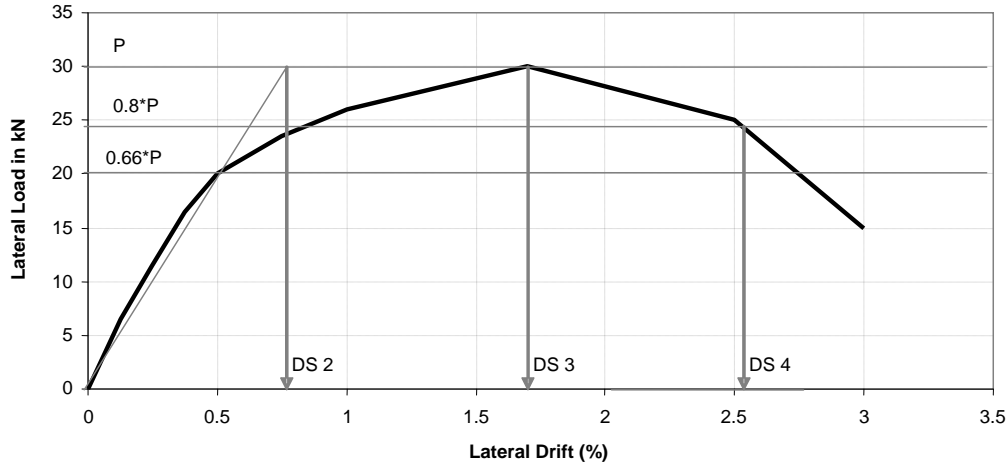
Figure 2.1. Details of adopted Damage States

The current study comprises of data from experimental investigation carried out over the last three decades. Test results of 180 slab-column connections were compiled for the development of fragility curve [Vijaya Narayanan, 2010]. For the current study only those specimens that failed through punching-shear or flexural-punching failure were considered. Median and Range of Drift computed for each damage state is summarized in Table 2.1

Table 2.1. Median and Range of Drift Associated with Different Damage States

System	Damage State	Number of data	Median	Range
RC non-ductile (TYPE A)	DS2	40	1.37%	0.64-2.63%
	DS3	77	1.97%	0.57-4.32%
	DS4	28	3.50%	0.90-5.76%
RC ductile (TYPE B & TYPE C)	DS2	22	1.80%	0.94-2.99%
	DS3	29	4.30%	2.50-7.60%
	DS4	13	4.85%	3.50-8.00%
PT non-ductile (TYPE D)	DS2	09	1.06%	0.47-2.10%
	DS3	09	2.39%	1.33-4.30%
	DS4	23	3.30%	1.80-6.00%
PT ductile (TYPE E)	DS2	09	1.53%	0.75-2.04%
	DS3	10	3.50%	2.80-3.98%
	DS4	15	5.45%	4.40-6.10%

3. FRAGILITY ANALYSIS

Statistically, fragility curves are probability distribution function that provides the probability of exceeding or experiencing any defined damage state. In most cases, the fragility function takes the form of cumulative log-normal distribution. Eqn. 3.1 provides the probability of drift capacity exceeding any damage state,

$$P(DS \geq ds_i \mid DC = dc) = \Phi\left[\frac{Ln(dc) - Ln(\overline{dc})}{\sigma_{Lndc}}\right]$$ (3.1)

where $P(DS \geq ds_i \mid DC = dc)$ is the probability of experiencing or exceeding the damage state i, $\overline{dc}$ is the median drift at which the damage state i was observed, σ_{Lndc} is the standard deviation of the natural logarithm of the dc, and Φ is the standard normal cumulative distribution function. In this

study, three different fragility curves for slab-column connections have been generated and they are as follows,

Case 1: Fragility curves as a function of drift without accounting for specimen-to-specimen variability and epistemic errors,
Case 2: Fragility curves as a function of drift accounting for specimen-to-specimen variability but without correction for epistemic error, and
Case 3: Fragility curves as a function of drift accounting for specimen-to-specimen variability and with appropriate corrections for epistemic error.

3.1 Fragility curves as a function of drift without accounting for specimen-to-specimen variability and epistemic errors

In this section, fragility curves were generated assuming drift to be an independent parameter. Fragility curve for each type of slab-column connection, and for each damage state, is arrived by substituting the respective median drift and standard deviation of natural logarithm of drift in Eqn. 3.1. Fragility curve for RC non ductile system (TYPE A) at damage state 3 is as shown in Fig. 3.1. In order to ascertain the validity of lognormal fit for developed cumulative frequency distribution, Kolmogorov-Smirnov (K-S) goodness-of-fit test was performed. The hypothesis that the assumed cumulative distribution adequately fits the empirical data is accepted if all the data points lie between the two grey lines. Based on Fig. 3.1, it can be inferred that for RC non-ductile slab-column connection there is a 30% probability of exceeding DS3 for an imposed drift of 1.5%.
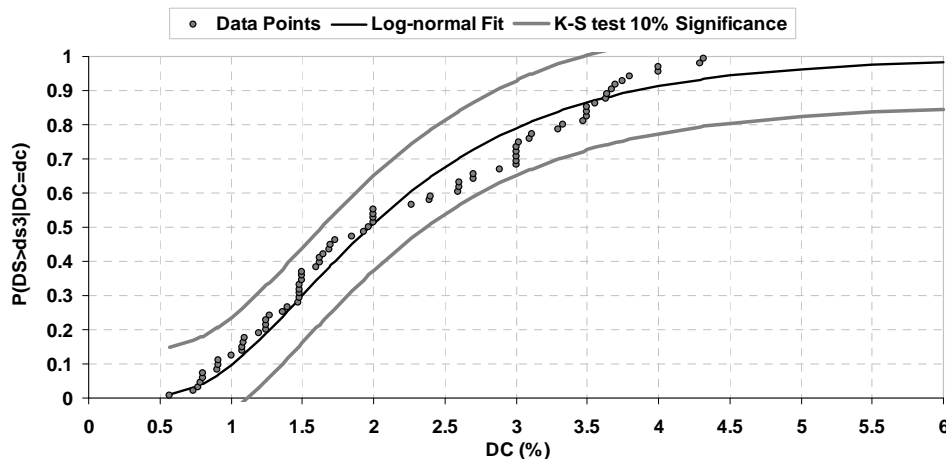

Figure 3.1. Probability of experiencing damage state 3 for RC non-ductile system.

3.2 Fragility curves as a function of drift accounting for specimen-to-specimen variability but without correction for epistemic error

In the past, researchers have observed that incorporating specimen to specimen variability provides better estimate of vulnerability [Aslani *et al.*, 2005]. Based on past research, it is evident that the drift capacities of slab-column connections are largely dependent on gravity shear ratio (V_g/V_c) imposed over the connection [Pan and Moehle 1989, Megally *et al.*, 1994, Kang *et al.*, 2006 and 2007]. Gravity shear ratio is defined as the ratio of shear force imposed as a result of gravity load over the slab-column critical section (V_g) to the total shear capacity of the critical section (V_c). Consequently, for the current study, gravity shear ratio for slab-column connection was considered to be the system parameter, i.e., the deformation capacity of the slab-column connection is assumed to be a function of gravity shear ratio, as shown in Eqn. 3.2. The function of the system parameter is to account for the specimen to specimen variability. Fragility curve generated accounting for specimen-to-specimen variability outlines the probability of experiencing a particular damage state as a function of drift capacity and gravity shear ratio of the connection.

$$dc = f(V_g / V_c) \tag{3.2}$$

where, dc and V_g/V_c refers to the drift and gravity shear ratio of the slab-column connection, respectively. Fig. 3.2, shows the variation of drift (DS3) for RC non-ductile slab-column connection (TYPE 1) as a function of gravity shear ratio. Boots strap analysis indicated significant correlation factor between the gravity shear, reaffirming the initial assumption to consider gravity shear ratio as system parameter. Formulation for the best fit line is given by Eqn. 3.3 In the proposed fragility curve, the formulation stated in Eqn. 3.3 was utilized for estimation of the median drift corresponding to each gravity shear ratio.

$$\overline{dc}_{DS3} = 1.24 + 2.38 \exp\left[-87.8\left(\frac{V_g}{V_c}\right)^{4.41}\right] \tag{3.3}$$

where, $\overline{dc}_{DS3}$ is the median drift associated with the damage state 3 and (V_g/V_c) is the gravity shear ratio. Through moving window analysis, the dispersions in logarithmic drift capacity were developed as a function of gravity shear ratio [Aslani et al., 2005]. To obtain a continuous function for variation of $\sigma_{Ln\,dc\,DS3}$ as a function of gravity shear ratio, a 2nd order function, as shown in Eqn. 3.4, was approximated from the data points generated through moving window analysis.

$$\sigma_{Ln\,dcDS3} = -0.876\left(\frac{V_g}{V_c}\right)^2 + 1.098\left(\frac{V_g}{V_c}\right) - 0.003 \tag{3.4}$$

where, $\sigma_{Ln\,dc\,DS3}$ is the logarithmic standard deviation of drift for damage state 3 and (V_g/V_c) is the gravity shear ratio as defined earlier. In order to estimate the probability of exceeding drift capacity inherent to damage state 4, the following ratio was computed,

$$\Gamma_{43} = \frac{dc_{DS4}}{dc_{DS3}} \tag{3.5}$$

where, dc_{DS4} and dc_{DS3} refers to drift corresponding to damage state 4 and damage state 3, respectively. The ratio can be construed as an amplification factor through which the drift at damage state 4 could be obtained as a multiple of drift at damage state 3. Eqns. 3.6 and 3.7 shows the formulation developed for the median and the logarithmic standard deviation, based on well-established statistical rules.
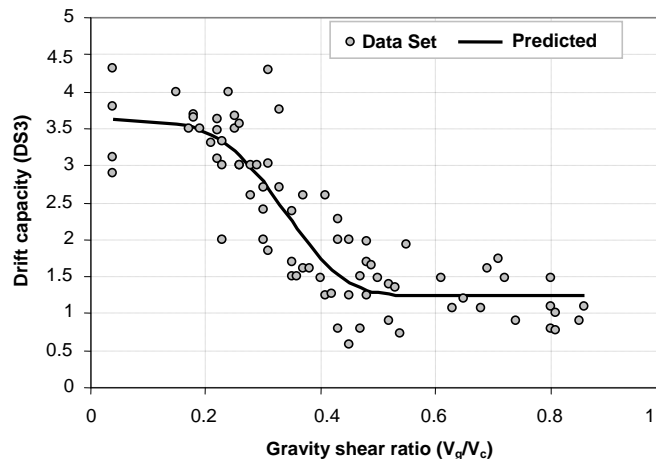

Figure 3.2. Variation of Drift capacity (DS3) with gravity shear ratio for RC non-ductile connections.

$$\overline{dc}_{DS4} = 1.22\overline{dc}_{DS3} \tag{3.6}$$

$$\sigma_{Lndc\,DS4} = \sqrt{\sigma^2_{Lndc\,DS3} + 0.08\sigma_{Lndc\,DS3} + 0.036} \tag{3.7}$$

where, $\sigma_{Lndc\,DS4}$ is the logarithmic standard deviation of the drift for damage state 4 and $\overline{dc}_{DS4}$ & $\overline{dc}_{DS3}$ refers to the median drift corresponding to damage states 4 and 3, respectively. Based on similar procedure outlined above, probability of exceeding damage state 2 was computed.

Eqns. for the generation of fragility curve for different types of slab-column connections, and for different damage states are as shown in Table 3.1. Due to insufficient data points, fragility curves pertaining to damage state 4 for RC ductile connections (TYPE B & TYPE C) and damage state 2, 3 and 4 for PT ductile connection were not generated.

3.3 Fragility curves as a function of drift accounting for specimen-to-specimen variability and with appropriate corrections for epistemic error

Random observations due to uncertainty induced as a result of lack of knowledge are termed as epistemic uncertainty [Bradley, 2010]. In this section, fragility curve generated in section 3.2 are corrected to account for epistemic uncertainty. For the current study, confidence interval developed by Crow et al [1960] for log-normal data set was used to estimate the upper and lower bound of median and logarithmic standard deviation, as shown in Eqn.s 3.8 and 3.9, respectively.

Table 3.1. Median and Logarithmic standard deviation of drift for different types of slab-column connection and for different damage states

System	Damage State	Median	Logarithmic standard deviation of drift
RC non-ductile (TYPE A)	DS2	$\overline{dc}_{DS2} = 0.57\overline{dc}_{DS3}$	$\sigma_{Lndc\,DS2} = \sqrt{\sigma^2_{Lndc\,DS3} - 0.385\sigma_{Lndc\,DS3} + 0.121}$
	DS3	$\overline{dc}_{DS3} = 1.24 + 2.38\exp\left[-87.8\left(\dfrac{V_g}{V_c}\right)^{4.41}\right]$	$\sigma_{Lndc\,DS3} = -0.876\left(\dfrac{V_g}{V_c}\right)^2 + 1.098\left(\dfrac{V_g}{V_c}\right) - 0.003$
	DS4	$\overline{dc}_{DS4} = 1.22\overline{dc}_{DS3}$	$\sigma_{Lndc\,DS4} = \sqrt{\sigma^2_{Lndc\,DS3} + 0.08\sigma_{Lndc\,DS3} + 0.036}$
RC ductile (TYPE B)	DS2	$\overline{dc}_{DS2} = 0.55\overline{dc}_{DS3}$	$\sigma_{Lndc\,DS2} = \sqrt{\sigma^2_{Lndc\,DS3} - 0.19\sigma_{Lndc\,DS3} + 0.018}$
	DS3	$\overline{dc}_{DS3} = 4.56 - 2.13\left(\dfrac{V_g}{V_c}\right)$	$\sigma_{Lndc\,DS3} = -0.862\left(\dfrac{V_g}{V_c}\right)^2 + 0.621\left(\dfrac{V_g}{V_c}\right) - 0.061$
	DS4	-	-
RC ductile (TYPE C)	DS2	$\overline{dc}_{DS2} = 0.45\overline{dc}_{DS3}$	$\sigma_{Lndc\,DS2} = \sqrt{\sigma^2_{Lndc\,DS3} - 0.33\sigma_{Lndc\,DS3} + 0.036}$
	DS3	$\overline{dc}_{DS3} = 9.58 - 7.83\left(\dfrac{V_g}{V_c}\right)$	$\sigma_{Lndc\,DS3} = 0.72\left(\dfrac{V_g}{V_c}\right) - 0.16$
	DS4	-	-
PT non-ductile (TYPE D)	DS2	$\overline{dc}_{DS2} = 0.34\overline{dc}_{DS4}$	$\sigma_{Lndc\,DS2} = \sqrt{\sigma^2_{Lndc\,DS4} - 0.35\sigma_{Lndc\,DS4} + 0.212}$
	DS3	$\overline{dc}_{DS3} = 0.74\overline{dc}_{DS4}$	$\sigma_{Lndc\,DS3} = \sqrt{\sigma^2_{Lndc\,DS4} - 0.31\sigma_{Lndc\,DS4} + 0.072}$
	DS4	$\overline{dc}_{DS4} = 6.87 - 8.31\times\left(\dfrac{V_g}{V_c}\right)$ for $\left(\dfrac{V_g}{V_c}\right) \leq 0.55$ $\overline{dc}_{DS4} = 2.3$ for $\left(\dfrac{V_g}{V_c}\right) \geq 0.55$	$\sigma_{Lndc\,DS4} = -1.14\left(\dfrac{V_g}{V_c}\right)^3 - 2.16\left(\dfrac{V_g}{V_c}\right)^2 + 1.21\left(\dfrac{V_g}{V_c}\right) - 0.037$

$$\overline{dc}.\exp\left[\pm z_{\alpha/2}\frac{\sigma_{\ln dc}}{\sqrt{n}}\right] \tag{3.8}$$

where, $z_{\alpha/2}$ is the value in the standard normal distribution such that the probability of random deviation numerically greater than $z_{\alpha/2}$ is α, and n is the number of data points. $\sigma_{\ln dc}$ refers to the logarithmic standard deviation associate with the drift capacity pertaining to each damage state.

$$\left[\frac{(n-1)\sigma^2_{\ln dc}}{x^2_{\alpha/2,n-1}}\right]^{1/2} \text{ and } \left[\frac{(n-1)\sigma^2_{\ln dc}}{x^2_{1-\alpha/2,n-1}}\right]^{1/2} \tag{3.9}$$

where, $x^2_{\alpha/2,n-1}$ is the inverse of x^2 distribution with n-1 degree of freedom and probability of occurrence of $\alpha/2$, similarly $x^2_{1-\alpha/2,n-1}$ is the inverse of x^2 the distribution with n-1 degree of freedom and a probability of occurrence of $1-\alpha/2$.

4. COMPARISON OF SEISMIC VULNERABILITY OF SLAB-COLUMN CONNECTIONS

Prior to comparison of vulnerability of different types of slab-column connections, it is imperative that the fragility curves generated based on three cases (*Case 1, Case 2 & Case 3*) are compared in order to understand the variation in the probabilistic estimate stemming from the fundamental assumption and the degree of uncertainty are addressed. Comparison of probability of exceedence for fragility curve generated using *Case 1* (refer Fig. 3.1), *Case 2* (refer Fig. 4.1) and *Case 3* (refer Fig. 4.2) is summarized in Table 4.1. Fig. 4.1 shows fragility curves corresponding to damage state 2, 3 and 4, for a connection of TYPE A with different gravity shear ratio, generated accounting for specimen-to-specimen variability. Fig. 4.2 shows the generated fragility curve corresponding to damage state 3, for a connection of TYPE A with different gravity shear ratio, accounting for both specimen-to-specimen variability and correction for epistemic error. Based on the tabulated (Table 4.1) probability of exceedance value, it is evident that the exceedence value obtained from *Case 1* is significantly different from the exceedence value obtained from *Case 2* and *Case 3*. Since, *Case 2* accounts for the variability of the specimen, the exceedence value obtained from *Case 2* is deemed to be a better estimate than the exceedence value obtained from *Case 1*. Exceedance values obtained from *Case 3* provides an upper and lower bound estimates based on the unknown parameters which might affect the probability estimates. Consequently, the range of values prescribed by *Case 3* is considered better than both *Case 2* and *Case1*.

It is evident that the vulnerability of the connection increases with the increase in the gravity shear ratio imposed on the connection irrespective of the type of slab-column connection. For a gravity shear ratio of *0.2, 0.35* and *0.5,* maximum drift that can be imposed on the connection before the connection reaches damage state 3 is *3.3, 2.1* and *1.2,* respectively (Fig. 4.1). Further, for all types of slab-column connection considered, it is observed that the area encompassed between the upper and lower bound decreases with the increase in gravity shear ratio (Fig. 4.2). The slope of the fragility curve is observed to increase gradually with the increase in the gravity shear ratio, implying that the sensitivity of the connection to reach a particular damage state, with the slightest change in drift, is higher in the case of connections with higher gravity shear ratio. Variation in the drift capacity with different type of connection, at damage state 3 corresponding to *5%* probability of exceedence is as shown in Fig. 4.3. The plot reaffirms the enhanced drift capacity of ductile connection as compared to non-ductile connections. Drift capacity and the fragility of non-ductile connection were observed to saturate between a gravity shear ratio of *0.45* and *0.55*. On the contrary no such saturation was observed for the ductile connections. Similar observations were made for all the other damage states.

Table 4.1. Comparison of probability of exceedence based on fragility curves using Case 1, 2 and 3.

System	Drift	Case 1 : *Refer Fig. 3.1*	Case 2 : *Refer Fig. 4.1*	Case 3 : *Refer Fig. 4.2*
RC non-ductile (TYPE A)	*1.5%*	Immaterial of the gravity shear ratio, the probability of exceedence is *30%*	For connection with gravity shear ratio *0.2, 0.35* and *0.5,* the probability of exceedence is *0.7%, 7%* and *70%,* respectively	For connection with gravity shear ratio *0.2, 0.35* and *0.5,* the probability of exceedence ranges between is *0 to 1%, 3 to 20%* and *55 to 83%,* respectively
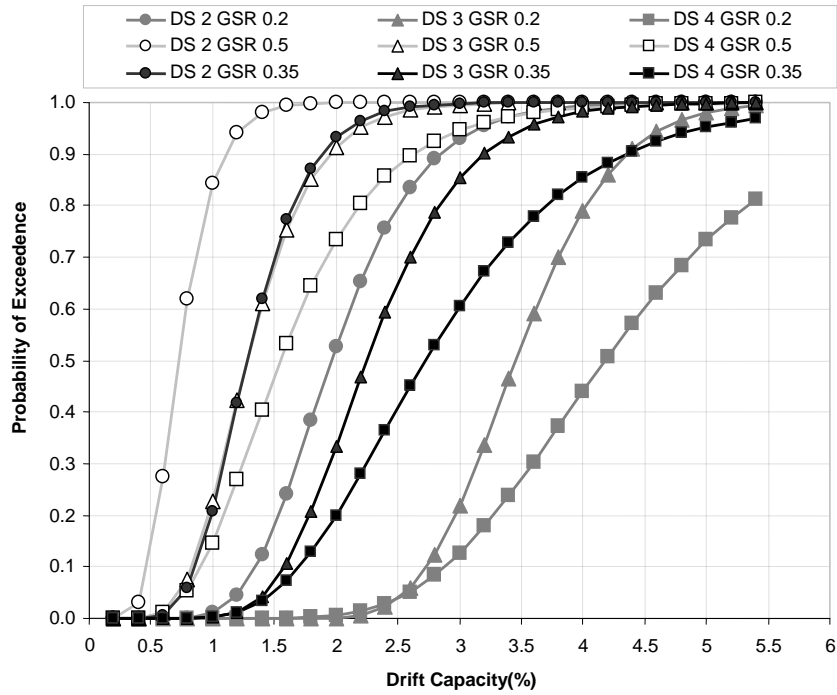
Figure 4.1. Fragility curves for RC non-ductile connection (TYPE A), with different gravity shear ratio, generated after accounting for specimen-to-specimen variability
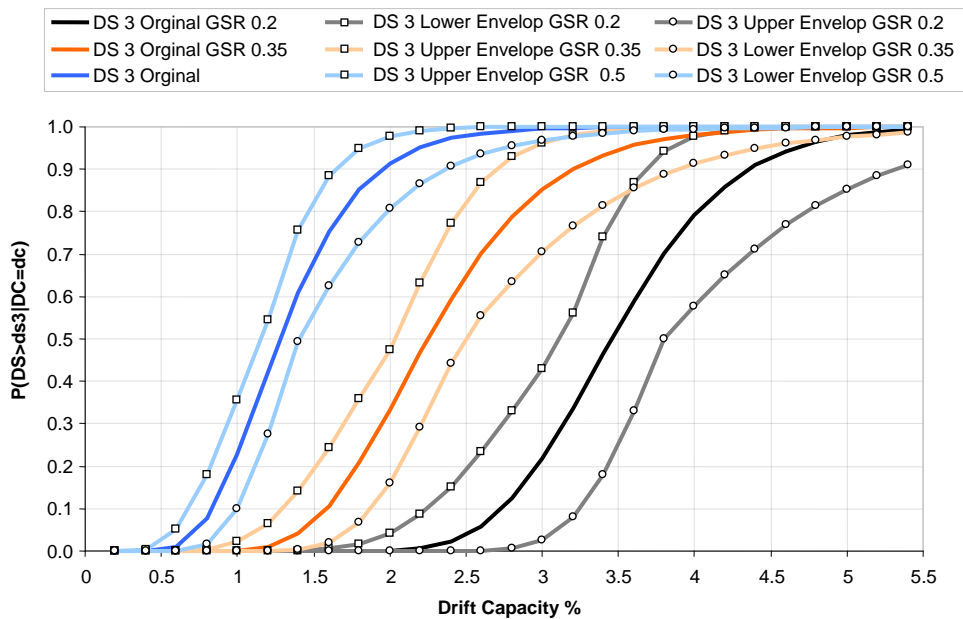

Figure 4.2. Fragility curves for RC non-ductile connection (TYPE A), with gravity shear ratio of 0.4, generated after accounting for specimen-to-specimen variability and correction for epistemic uncertainty
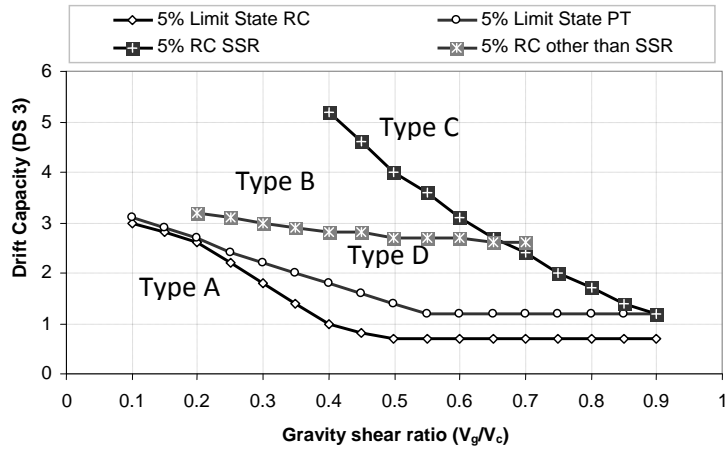
Figure 4.3. Variation in Drift, corresponding to 5% probability of exceedence pertaining to DS 3, with increase in gravity shear ratio

A comparison of the fragility curve, corresponding to damage state 3, developed for different type of connection for the same gravity shear ratio of *0.4* is as shown in Fig. 4.4. Irrespective of the damage states, the fragility curves for the ductile connections were observed to be lower than their non-ductile counterparts. Further, within the ductile system, connection with SSR as shear reinforcement indicate an enhanced drift capacity and lesser vulnerability as compared to connection with any other type of shear reinforcement. On other hand, within the non-ductile system, PT non-ductile system was observed to be having higher drift capacity and lower fragility as compared to RC non-ductile system. The difference in the fragility curves between RC and PT non-ductile connection for damage states 2, 3 and 4 is shown in Fig. 4.5. The difference in the drift capacities computed at any probability of exceedence, between the RC non-ductile and PT non-ductile connection is observed to increase, with the increase in the damage state. Based on this observation, it may be concluded that the provision of PT slab system may not help in improving the drift capacity associated with lower damage state, but would definitely help in enhancing the drift capacities for higher damage states. Similar observations were noted while comparing the drift capacities of RC non-ductile connection and RC ductile (SSR) connection.
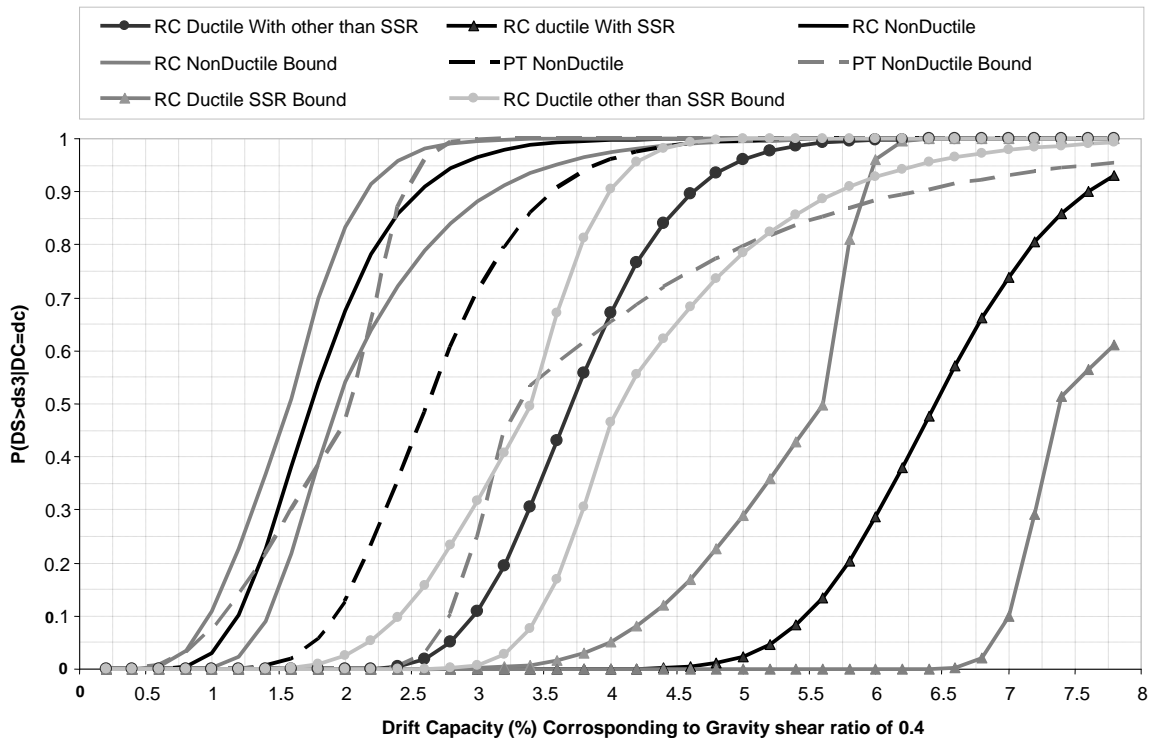

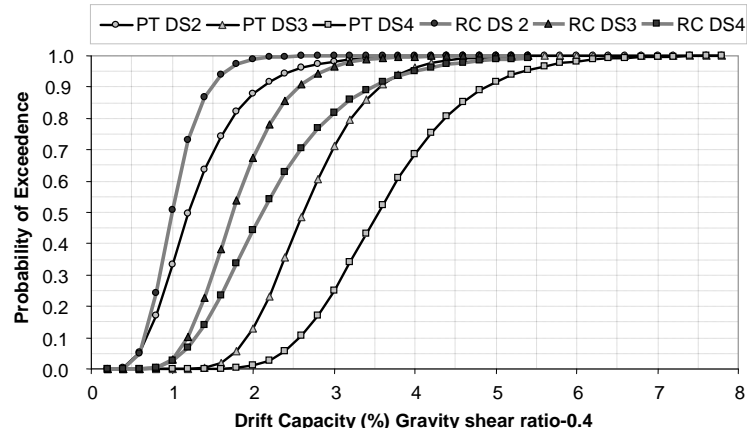**Figure 4.4.** Comparison of the fragility of different type of connections for damage state 3

Figure 4.5. Comparison between fragility curve between RC and PT non-ductile connection at damage state 2, 3 and 4

5. CONCLUDING REMARKS

Fragility curve developed assuming drift capacity of the connection to be independent of any system parameter revealed a significant standard deviation associated with the prediction, which could eventually overestimate or underestimate the probability of failure. The effects of specimen-to-specimen variability and epistemic errors are included in fragility curves to reduce variability associated with the generation of fragility curves. Fragility curves for different connection has been developed and it was observed that with the increase in gravity shear ratio, the damage to the connection increased proportionally. The drift capacity of connections having gravity shear ratio greater than *0.45* and *0.55* for RC and PT non-ductile slab-column connection, respectively, were found to saturate, implying equal vulnerability of all connections exceeding the specified limits of gravity shear ratio. Further, for RC non-ductile connection, the drift capacity was observed to be very sensitive to changes in the gravity shear ratio within a window ranging from *0.2-0.5*. The performance of PT non-ductile connection was marginally better than the RC non-ductile connection. With the provision of shear reinforcement, the likelihood of shear failure has been observed to reduce significantly. Within the ductile system, the connection reinforced with SSR was observed to undergo lesser damage and has higher drift capacity as compared to the connection reinforced with any other type of shear reinforcement.

REFERENCES

Aslani, H. and Miranda, E. (2005). Fragility Assessment of Slab-Column Connecitons in Existing non-ductile reinforced concrete buildings. *Journal of Earthquake Engineering* **9:6**, 777-804.
Bradley, B.A. (2010). Epistemic Uncertainties in Component Fragility Functions. *Earthquake Spectra* **26:1**, 41-62.
Crow, E. L., Davis, G. A. and Maxfield, M. W. (1960). Statistics Manual, Dover Publication, New York.
Kang, T.H.-K., and Wallace, J.W.(2006). Dynamic Responses of Flat Plate Systems with Shear Reinforcement. *ACI Structural Journal*, **102:5**, pp. 763-773
Kang, T. J. K. and Wallsce, J. W. (2007). Punching of Reinforced and Post-Tensioned Concrete Slab-Column Connections. *ACI Structural Journal* **103:4**, 531-540.
Megally, S., and Ghali, A.(1994). Design Considerations for Slab-Column Connections in Seismic Zones. *ACI Structural Journal* **91:3**, 303-314.
Pan, A. and Moehle., J.P. (1989). Lateral Displacement Ductility of Reinforced Concrete Flat Plates. *ACI Structural Journal* **86: 3**, 250-258.
Vijaya Narayanan, A.R., (2010). Fragility Estimates and Safe Design Limits for RC and PT Flat Slab subjected to Latreral Drifts. Masters Thesis, Indian Institute of Technology Kanpur, India.